

# NONLOCAL MECHANICS OF NONEQUILIBRIUM SHOCK-WAVE PROCESSES

**Yu.I. Meshcheryakov<sup>1\*</sup>, T.A. Khantuleva<sup>2</sup>**

<sup>1</sup>Institute of Problems of Mechanical Engineering RAS, Saint-Petersburg, Russia

<sup>2</sup>Saint-Petersburg State University, Russia

\*e-mail: ym38@mail.ru

**Abstract.** Results of experimental research on shock loading of solid materials demonstrate that the revealed dependences of waveforms and threshold of the structure instability on strain-rate, target thickness and state of the material structure cannot be described in the framework of the conventional continuum mechanics. New concept of shock-wave processes in condensed matter is proposed on base of nonlocal theory of nonequilibrium transport which allowed a transition from the elastic medium reaction to the hydrodynamic one depending on the rate and duration of the loading. A new mathematical model of elastic-plastic wave is constructed to describe the elastic precursor relaxation and the plastic front formation taking into account the changing of material properties during the wave propagation. Analysis of experimental waveforms shows that for the shock-induced processes it is incorrect a priori to divide the components of stress and strain into elastic and plastic parts. The model allowed accounting for the inertial medium properties under short-duration loading and self-organization of new internal structures.

## 1. Introduction

In different regions of mechanics, the experimental researches of dynamic processes show a lot of common features which characterize an anomalous reaction of medium to an intense external action. Far from the thermodynamic equilibrium, transport processes are often accompanied by the formation of new multi-scale structures at mesoscopic scale level, such as shear bands, vortex structures, localized heterogeneities, velocity pulsations etc. The effects of self-organization observed in the target materials under study after shock loading [1-5] are determined not only by the material properties and its phase state but also by the loading and boundary conditions and by size and geometry of a system. The response to the high-rate external action begins to retard from the initial action and can be spread over space. The interaction between the structure elements causes the formed structures to evolve. The rate of the structure evolution and retarding responses to the actions could affect the relaxation characteristics of medium and lead to the system instability, fluctuations, to structure transformations, switching from one regime to another and to origin feedbacks. An influence of the individual factor among all the rest effects becomes indistinguishable because of the close-loops formed in the system. So, self-organization and self-regulation should be included into the mathematical model of an open system far from equilibrium to reveal indeterminacy effects.

At high-rate transport, the mean mass, impulse and energy densities are determined only in terms of the probability conception and don't entirely coincide with their definition near equilibrium in the framework of continuum mechanics. Unlike quasi-static processes well reproduced in experiments, reliability of experimental measurements for dynamic processes is

markedly decreased, so accumulation of sufficient statistical data on the process is impossible. The occurrence of oscillations and instabilities reduce the control opportunity and obstruct the system study.

Thus, an adequate description of nonequilibrium processes requires to go beyond the continuum mechanics limits and to develop a new approach at the junction of continuum mechanics, nonequilibrium thermodynamics and control theory.

In the paper, the experimental results on shock loading of solids (metals) are presented. Experimental researches on shock loading of metals show that, together with non-stationary waveforms, the important dynamic characteristics are the mass velocity variation, velocity defect and threshold of structural instability registered in real time [6-8]. The revealed relationships between the quantities testify multi-scale impulse and energy exchange accompanying the wave transport. The theoretical description of the shock-induced transport processes accompanied by the formation of new mesoscale structures is proposed. A complex of mathematical models developed on the basis of nonlocal theory of nonequilibrium processes allows the description of the medium behavior under dynamical loading outside the conception of continuum mechanics. By using the models, a problem of evolution of unsteady elastic-plastic wave initiated by the plane shock loading is solved. Comparison of the calculated waveforms with the experimental results elucidates specific features of material response to the shock loading which characterize dynamic loading unlike quasi-static one. The anomalous loss of the mass velocity amplitude in the wave propagation is explained by the energy exchange between macroscopic scale level and mesoscopic degrees of freedom. Due to the exchange processes, the material during high-rate deformation achieves a structure-unstable state in which there emerges a synergetic genesis of the three-dimensional eddy-wave pulsations observed in experiments.

## 2. Experiments on shock tests of solids

Although concept of mesomechanics has been introduced more than thirty year ago, it is not incorporated into theoretical studying of the shock-wave processes till present [9]. The diversity of mechanisms of impulse and energy exchange between degrees of freedom at different scale levels leads to the lack of general relationships linking the dynamic variables at macroscale with mesoscopic variables. At the same time, experiments on shock loading of solids show that the following measured quantities characterize the impulse and energy exchange between macro- and mesoscale levels: (i) mass velocity defect resulting from the impulse loss in the process of shock-induced structural transformations of material and (ii) mass velocity variation (square root of the mass velocity dispersion) resulting from the mass velocity pulsations. Experiments show that conventional opinion that 90-95 % of cold deformation work is transformed into heat, in case of dynamic deforming does not respond to reality [10]. Depending on strain-rate, only 35-50 % of dynamic plastic work is shown to be transferred into heat. The rest of the energy is stored in the material giving rise cracks, shear bands and other structural defects.

In the case of shock loading, determination of velocity defect is grounded on the independent measuring of the free surface velocity,  $U_{fs}$ , and the velocity of impactor,  $U_{imp}$ . Wherein, the velocity defect is determined as a difference between the impact velocity and the maximal free surface velocity at the plateau of compressive pulse:  $U_{def} = U_{imp} - U_{max}$ . As example, Figure 1 shows the free velocity profile,  $U_{fs}(t)$ , for 5 mm 30KHN4M steel target loaded at the impact velocity of 237 m/s. Figure 2a,b shows the dependencies of  $U_{max} = f(U_{imp})$  and  $U_{def} = f(U_{imp})$  for 30KHN4M steel target. The dependence  $U_{def} = f(U_{imp})$  consists of two parts: on the first segment ( $A'B'$ ) the mean value of the velocity defect  $U_{def}$  is small and almost constant, on the second segment ( $B'C'$ ) the velocity defect linearly grows as  $U_{def} \sim U_{imp}$ . At the impact velocity of 376 m/s there occurs an inflection point on the curve  $U_{max} =$

$f(U_{fs})$ , corresponding to a threshold of structural transition equal to  $U_{max} = U_{st} = 323.8$  m/s. Starting with the impact velocity of 376 m/s, the velocity defect begins to grow very fast (segment  $B'C'$  in Fig. 2b).

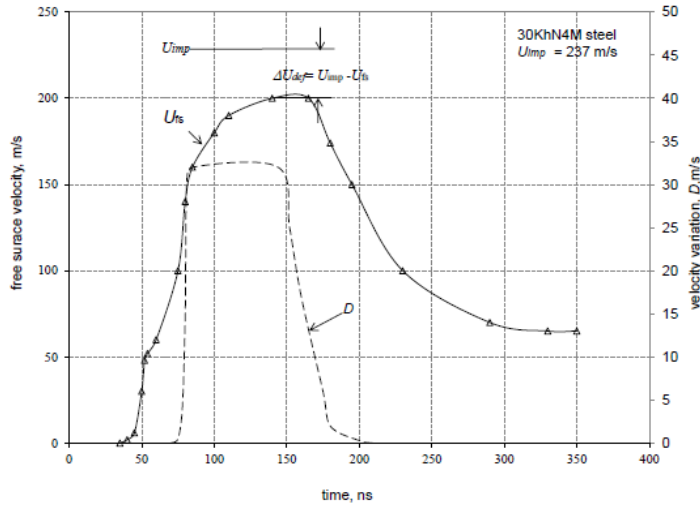


**Fig. 1.** Free surface velocity profile,  $U_{fs}(t)$ , and variation velocity profile,  $D(t)$ , for 5 mm 30KhN4M steel target loaded at the impact velocity of 237 m/s.

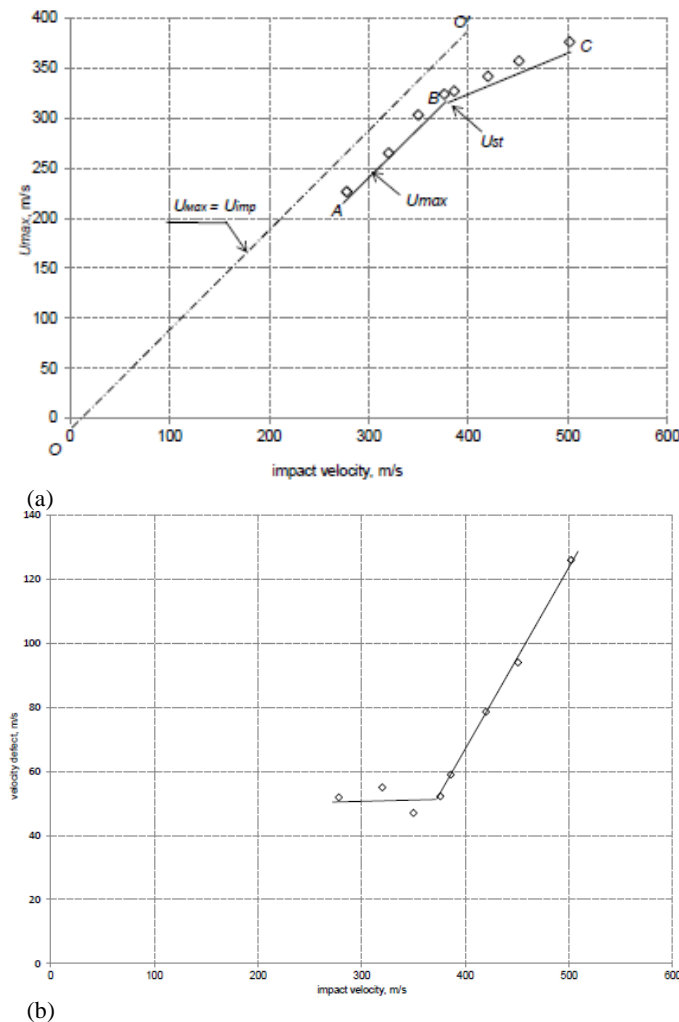


**Fig. 2.** Dependencies of maximum free surface velocity,  $U_{max}$ , (a) and velocity defect,  $U_{def}$ , (b) on the impact velocity for 30KHN4M steel.

Analogous behavior of the maximal free surface velocity for D16 aluminum alloy can be seen in Fig. 3a,b. Structural instability happens at the impact velocity of 382 m/s which corresponds to beginning the shock-induced dynamic recrystallization process [11, 12]. The velocity defect begins to increase at the impact velocity of 382 m/s, which testifies the increase of the energy expenses related to dynamic recrystallization.

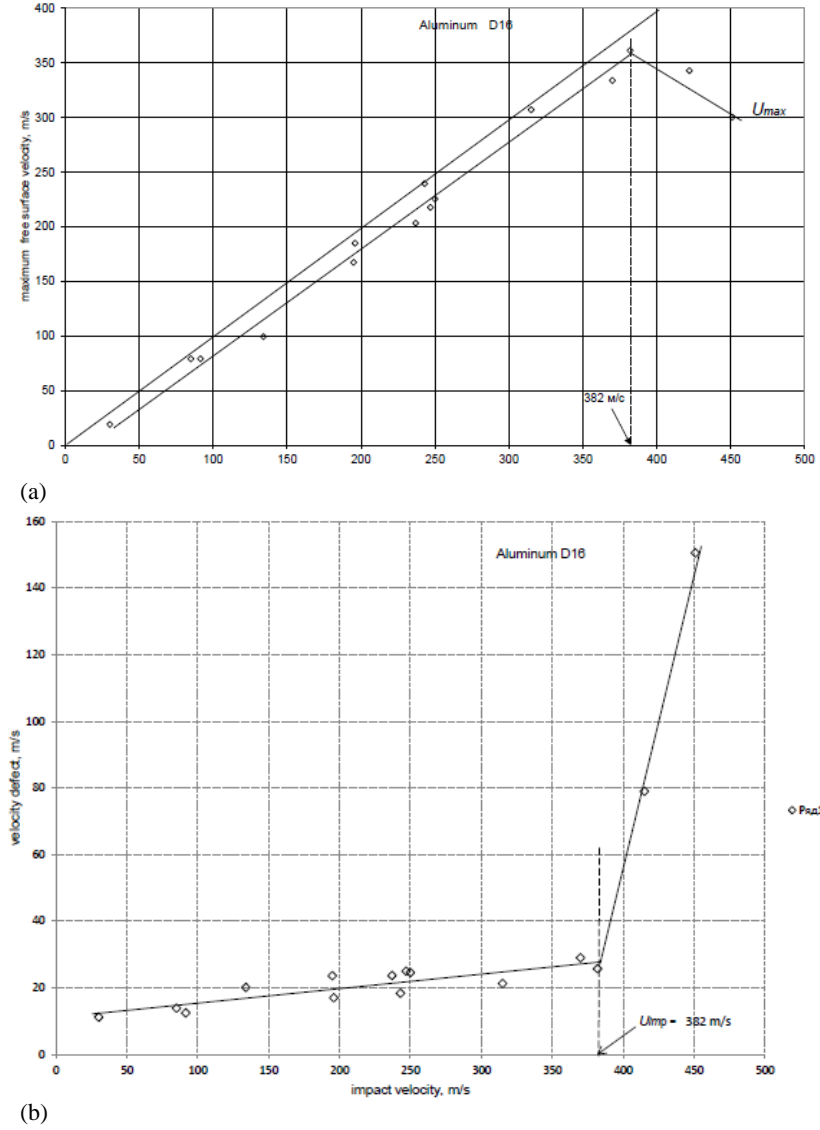


**Fig. 3.** Dependencies of maximum free surface velocity,  $U_{max}$ , (a)

and velocity defect,  $U_{def}$ , (b) on the impact velocity for D16 aluminum alloy.

Value of the velocity defect depends on initial state of material, strain-rate, tendency of material to structural and phase transformations and so on. For example, influence of initial structure on the macroscopic material response can be seen in Fig. 4 which shows the time-resolved free surface velocity profiles for two 5 mm 30KN4M steel targets of different structural states. The first kind of steel (1) has been subjected to standard thermo-mechanical processing (annealing at 250 °C) whereas the second kind of steel (2) was annealed at 450 °C. Both targets have been shocked at the impact velocity of 320 m/s. For the steel (1) the velocity defect equals to 10 m/s whereas for the steel (2), a structural transition occurred, which results in large value of the velocity defect equals to 160 m/s. That experiment shows that the initial state of material directly influences on the macroscopic response of material to shock loading.

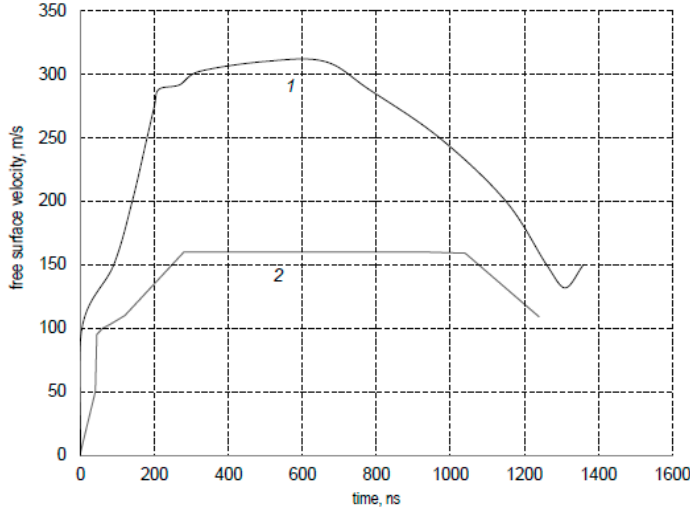


**Fig. 4.** Free surface velocity profiles,  $U_{fs}$ , for two kinds of 30KHN4M steel in different initial structural state before shock loading: 1) alloying at 250 °C, 2) alloying at 400 °C.

Below the critical strain-rate, the velocity defect depends on the strain-rate very weakly. Figure 5 shows the dependencies of the velocity defect on the impact velocity for two 5 mm targets of different kinds steel targets – 30KHN4M steel (1) and nitrogen steel (2). For the second kind of steel, the velocity defect remains invariable. Absence of the inflection point on the curve  $U_{def} = f(U_{fs})$  for this material means that the material was not subjected to a structural instability transition all over the region of impact velocities under consideration.

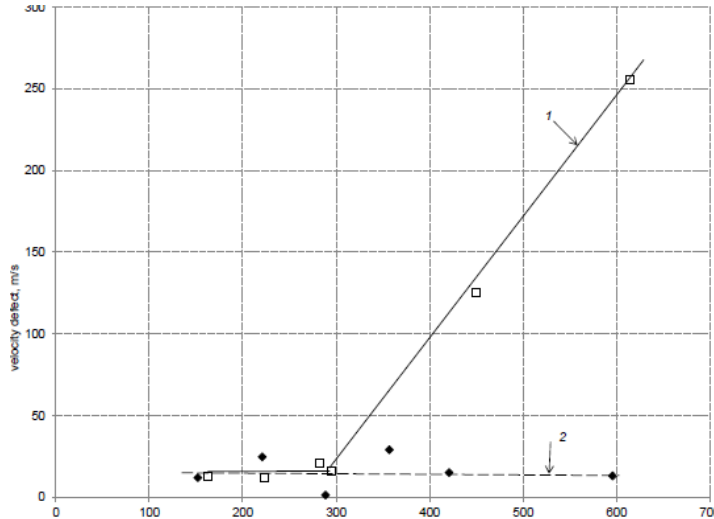


**Fig. 5.** Dependencies of the velocity defect,  $U_{def}$ , on the impact velocity for perlite steel target (1) and for nitrogen steel target (2).

Figure 6a,b shows a different situation observed for the free surface velocity profiles in AMg-6 aluminum alloy targets at the impact velocities of 178 m/c and 187 m/s. In Figure 6a maximal amplitude of compressive pulse equals to the impact velocity (double free surface velocity). Figure 6b shows that instead of the expected value of 187 m/s, the registered value of the free surface velocity equals to 116 m/s. It means that between the impact velocity 178 m/s and 187 m/s a transition from evolutional stage of dynamic straining to catastrophic stage (break of the interference signal is marked by symbol A) happens, which results in increase of the velocity defect up to 74 m/s. This result evidences that valuable part of impulse and energy is expended on the internal processes of structure formation.

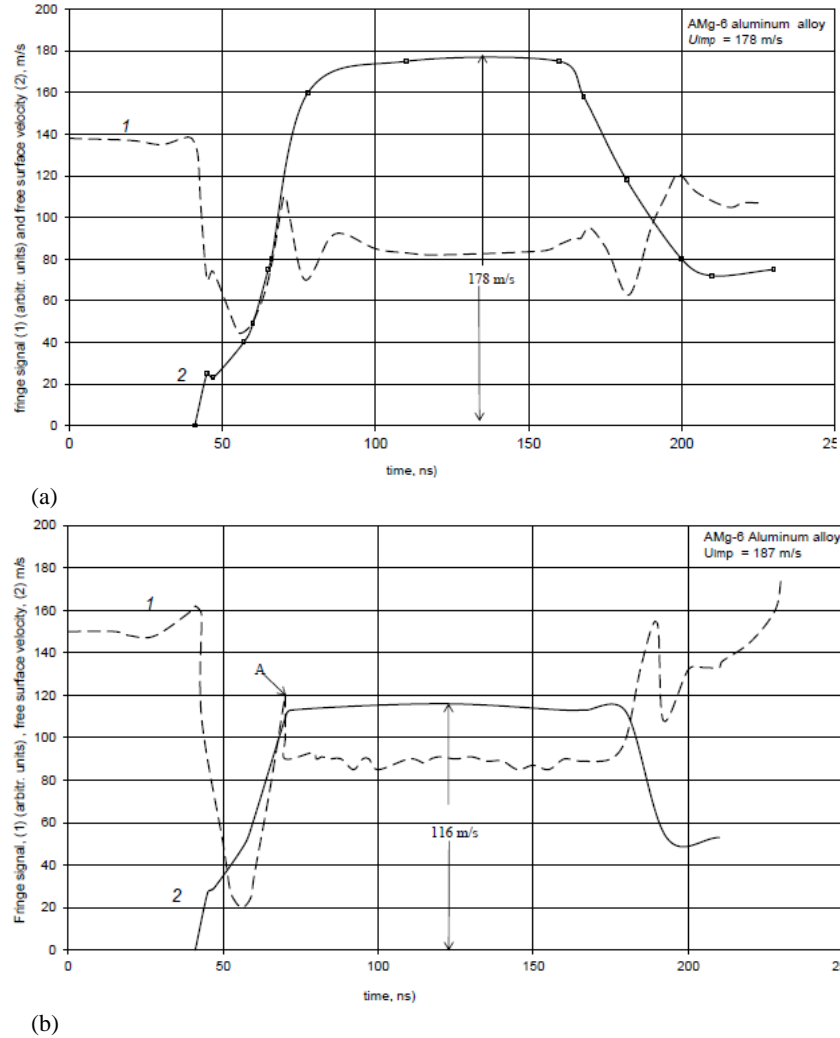


**Fig. 6.** Fringe signals (1) and free surface profiles (2) for AMg-6 aluminum alloy targets shocked at the impact velocity of 178 m/s, (a), and 187 m/s, (b).

Since the velocity defect is generated by the exchange processes accompanying the relaxation of deformed medium, its value changes in the shock wave propagation. Figure 7a,b shows two time-resolved free surface velocity profiles for 30KhN4M steel targets of the identical composition and identical initial structural state but of different thickness (5 mm and 10 mm), both loaded under close impact velocities of 318 m/s and 320 m/s. With increasing the target thickness, the velocity defect grows from 47 m/s to 125 m/s.

The examples show that macroscopic response of material to shock loading depends both on the initial state of material, loading conditions and thickness of target. These facts can be explained only taking into account the nonequilibrium multi-scale processes of energy and impulse exchange inside the shock wave. Evidently, conventional approaches based on the concept of continuous structureless medium are invalid to describe such processes. In this situation, there is a need for a new theoretical approach which would be able to describe the high-velocity processes considering the whole complex of accompanying effects.

### 3. Nonequilibrium effects in condensed matter under dynamic loading

It is commonly known that under shock loading at pressures below the elastic limit the changeless elastic waveforms propagate, the process of the pulse propagation is reversible and isn't accompanied by mass transport. The medium behavior is entirely described by the elastic modules in the framework of the conventional medium model of the elastic solid.

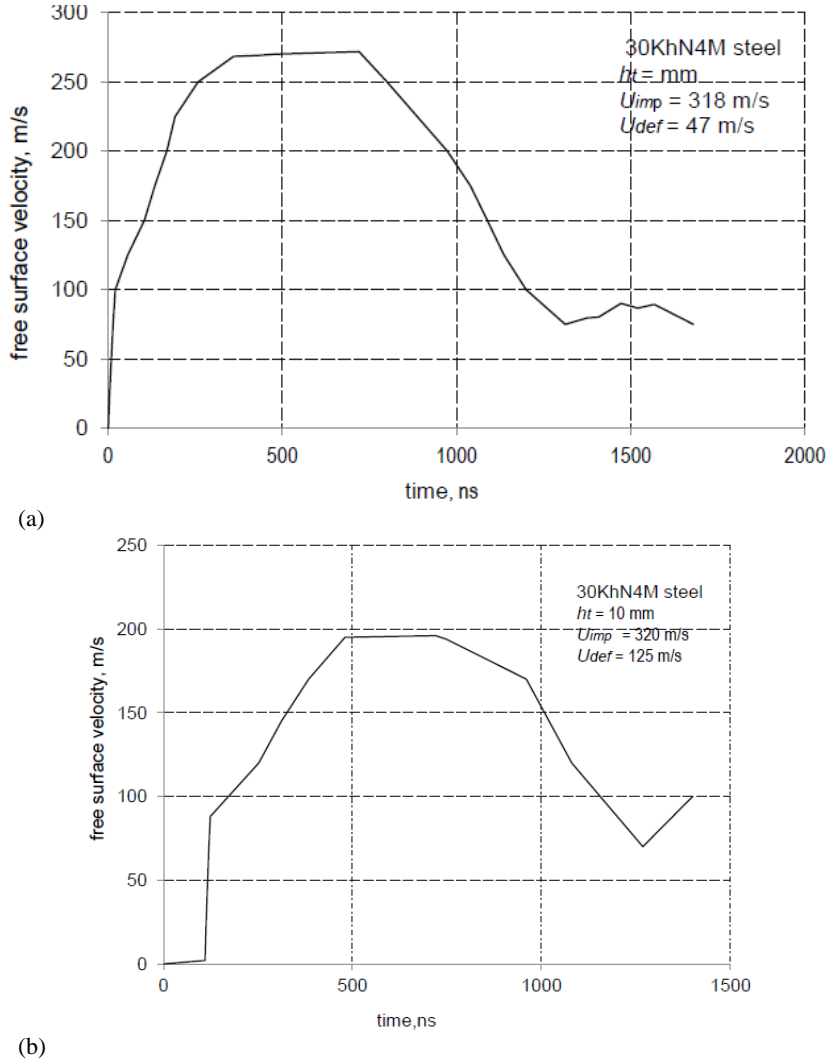


**Fig. 7.** Free surface velocity profiles,  $U_{fs}$ , for 5 mm (a) and 10 mm (b) 30KHN4M steel targets shocked at the impact velocities of 318 m/s and 320 m/s, respectively.

Beyond the elastic limit, the mass transportation becomes irreversible, the waveform changes during propagation and the so-called two-wave structure of elastic-plastic wave is formed. Lastly, under long-time loading, any medium manifests a hydrodynamic behavior. The transport processes become irreversible because of the energy dissipation into heat. At the intermediate stage, a medium shows both elastic and hydrodynamic behavior. Elastic modules depend on strain-rate whereas viscosity and relaxation time are determined by size and geometry of the system. Under these conditions, the medium constants become functionals of transport processes whereas conventional models of elastic body and/or viscous liquid appear to be incorrect. Such transient processes are not described within continuum mechanics concepts. In transient processes, deformation cannot be correctly subdivided into elastic and plastic components as well as phase and group velocities cannot be properly defined for non-stationary waves [13, 14].

From the standpoint of continuum mechanics, the reaction of condensed matter to the dynamic load is anomalous as far as determined by the nonequilibrium transport processes beyond the validity of the continuum mechanics concept. These processes are accompanied by the effects of collective interaction of the medium elements, which result from inertia forces instead of the interaction potential. For the shock loading such characteristics as a rate of loading and duration of pulse play a principal role. As result, dynamic properties of medium depend on the loading regime and can essentially differ from the quasi-static ones

[15, 16]. Moreover, the medium state inside a wave can be changing during its propagation and, in turn, can change the wave front shape. The propagation of unsteady elastic-plastic waveforms is the transient nonequilibrium process which cannot be described by differential models.

In the present paper, an integral model of impulse transport is used to describe such transient processes. This model is developed within nonlocal transport theory [17-24] and proves to be free from enumerated defects.

#### 4. Nonlocal theory of nonequilibrium processes

From the viewpoint of nonequilibrium statistical mechanics, in case of arbitrary deviation from equilibrium state, any scale level of averaged description of a system is incomplete. So, one of the most constructive results of nonequilibrium statistical mechanics is a proof of the fact that equations describing a behavior of nonequilibrium statistical system in terms of incomplete set of variables cannot be differential, i.e. local both in the space and time [25-29]. A fruitful statistic-mechanical method to describe nonequilibrium transport processes of mass, impulse and energy had been proposed by D.N. Zubarev [28, 29]. The obtained within the approach relationships between conjugate fluxes  $\mathbf{J}(\mathbf{r}, t)$  and macroscopic density gradients of impulse and energy  $\mathbf{G}(\mathbf{r}, t)$  are integral both in space and time. They include relaxation transport kernels  $\mathcal{R}(\mathbf{r}, \mathbf{r}', t, t')$ , which generalize the transport coefficients to nonequilibrium conditions

$$\mathbf{J}(\mathbf{r}, t) = \int_{-\infty}^t dt' \int_V d\mathbf{r}' \mathcal{R}(\mathbf{r}, \mathbf{r}', t, t') \mathbf{G}(\mathbf{r}', t'). \quad (1)$$

Unlike the transport coefficients, the relaxation transport kernels are nonlinear functionals of macroscopic densities. Being projections of nonequilibrium distribution in the phase space of statistical system on configuration space, the kernels describe spatiotemporal correlations of macroscopic density fields. Since nonequilibrium states result from arbitrary external action, the transport kernels are unknown in general case. However, the presence of correlations in Eq. (1) indicates to an opportunity to consider the collective effects in condensed matter in the framework of the integral model. For the high-rate shock-wave processes when mechanical energy hasn't time to dissipate into heat, the cross processes in Eq. (1) can be neglected.

In the limiting cases of frozen and completed relaxation of the translational degrees of freedom, as it will be demonstrated below, the relaxation kernels characterize elastic and hydrodynamic reaction of medium, respectively. In both limits, the medium behavior is described by differential equations of continuum mechanics. Hyperbolic transport equations at the initial stage are replaced by parabolic equations at the final hydrodynamic stage of relaxation. In transient regimes, where collective effects and structure formation occur, the transport equations become integral-differential. In general case, any explicit form of the integral kernels is unknown. Attempts to construct empiric models of the integral kernels led to coarse models which could not satisfy boundary conditions. These obstacles discourage the use of nonlocal models in practical tasks.

On the basis of the nonlocal and retarded transport equations obtained within the nonequilibrium statistical method one of authors of the present paper proposed a new universal approach based on a self-consistent nonlocal theory of nonequilibrium transport processes to consider transport processes in open systems [17-24]. Within the theory, the mathematical model of the relaxation transport kernel contains parameters evolving in time and characterizing the scale of internal structure. In order to complete the model nonlocal equations, the theory of special kind nonlinear operator systems is applied [30, 31]. Cybernetic methods developed within the control theory of adaptive systems via close-loops

[32] are used to govern the evolution of the medium structure. Like in quantum mechanics, the boundary conditions for the model equations lead to discretization of scale spectrum of internal structure (structuration of system). By means of the structure parameters, the boundary problem formulation for the nonlocal equations becomes self-consistent: transport process depends on the structure of a system whereas the structure, in turn, is determined by the transport process itself. The close-loops between the structure evolution and the regime of loading are incorporated in the model. Only such multi-disciplinary approach at the crossroads of mechanics, physics and cybernetics leads to the closed self-consistent formulation of boundary problems for nonequilibrium transport processes in open systems. The approach allows a prediction of the dynamic medium properties under high-rate loading conditioned by the evolution of the inner medium structure. Successful description of the experimentally discovered effects within the nonlocal transport theory is shown to open a principally new opportunities to develop modern technologies in order to obtain materials with specified inner structure.

## 5. Nonlocal model of the impulse transport

The problem on the plane elastic-plastic wave propagation in condensed medium is considered. The impulse transport is initiated by a plane shock on the medium surface at a velocity  $V_0 \ll C$ .  $C$  is the longitudinal sound velocity determined by relationship  $\rho C^2 = K + \frac{4}{3}G$  in which  $\rho$  is the medium density,  $K$ ,  $G$  are the elastic compression and shear modules respectively. Elastic waves propagate at the phase velocity  $C$  without mass transportation. Beyond the elastic limit the waveforms consist of two fronts: elastic precursor propagating at the phase velocity  $C$  and plastic front propagating at the group velocity  $C^{pl} < C$ . Inside the plastic part of the waveform, the mass transport at the mass velocity  $v \ll C$  takes place. It is the irreversible mass transport that responds for the plastic deformation of material. Non-stationary waveforms can blur during propagation due to the medium dispersion, and therefore the velocity of uni-axial impulse transport cannot be a priori divided into two parts  $u = dx/dt = C^{pl} + v$ . At a distance from the shock surface, when pulses of moderate intensity propagate in solids at the constant group velocity  $C^{pl}$ , the mass velocity is determined correctly.

The medium state after such shock slightly deviates from the undisturbed one:  $\rho = \rho_0 + \rho_1$ ,  $\rho_0 = const$ ,  $\rho_1/\rho_0 \sim v/C \ll 1$ ,  $\rho_1$  is the density deviation. The longitudinal impulse flux component  $J_{xx} = J_0 + J_1$ ,  $J_0 = \rho_0 C^2 = const$  (it will be shown further) also contains a deviation  $J_1$  related to the induced stress. In the linear approximation with respect to the parameter  $v/C \ll 1$  equations of mass and impulse transport take a form

$$\frac{1}{\rho_0} \frac{\partial \rho_1}{\partial t} + \frac{\partial v}{\partial x} = 0, \quad (2)$$

$$\rho_0 \frac{\partial v}{\partial t} + \frac{\partial J_1}{\partial x} = 0. \quad (3)$$

If  $J_1 = \rho_1 C^2$  the set (2)-(3) results the wave equation for the elastic wave propagation with stationary waveform

$$\frac{\partial^2 v}{\partial t^2} - C^2 \frac{\partial^2 v}{\partial x^2} = 0. \quad (4)$$

However, beyond the elastic limit the two-front waveform evolves due to the relaxation of

shear degrees of freedom at the volume relaxation frozen. The elastic precursor is relaxing and plastic front is retarding in the wave propagation. At present there is no one adequate mathematical model for non-stationary wave propagation including the elastic-plastic transition.

Within the nonlocal theory of nonequilibrium transport processes [17-24] both relaxation effects and collective interactions can be taken into account by means of spatiotemporal correlation function  $\mathfrak{J}(x,x';t,t')$  incorporated as a kernel into the integral relationship between longitudinal stress component  $J_1(x,t)$  and the strain-rate  $\dot{\epsilon} = -\frac{\partial u}{\partial x}$

$$J_1(x,t) = -\rho_0 C^2 t_r \int_0^{\omega(t)} \frac{dt'}{t_r} \int_0^{\Omega(t)} \frac{dx'}{l_r} \mathfrak{J}(t,t';x,x';t_r,l_r) \frac{\partial v}{\partial x'}, \quad (5)$$

$$\omega(t) = \begin{cases} t, & t < t_R \\ t_R, & t \geq t_R \end{cases} \quad \Omega(t) = \begin{cases} Ct, & Ct < L \\ \Gamma, & Ct \geq L \end{cases}$$

Here  $t_R$  is typical loading time (force acts over a period  $t_R$ ) that is not included in conventional deformation models,  $L$  is typical distance from the impact surface (target thickness). The impulse relaxation kernel  $\mathfrak{J}$  depends on the parameters: typical shear relaxation time  $t_r$  and length  $l_r = Ct_r$  (all perturbations consider to propagate at the velocity  $C$ ). Shear relaxation is irreversible process whereas the volume one going much slower, should be considered frozen. In general case, the dynamic processes cannot be a priori divided into reversible and irreversible parts. Just the same applies to the division into elastic and plastic parts of stress-strain dependences.

Substitution of the relationship (5) into the impulse transport equation (3) results in integral-differential equation respectively the mass velocity inside non-stationary elastic-plastic wave. Unlike differential wave models, the integral relationship (5) determines the stress component  $J_1(x,t)$  at a spatiotemporal point by the strain-rate history all over the wave. Due to the inertial and relaxation effects the pulse duration can essentially exceed the loading time  $t_R$ . So, during the loading, impulse accumulates in the medium and relaxes after loading. That is why the upper limits in the integral relationship (5) are variable during the loading and fixed after it. Near equilibrium, relaxation always goes monotonously whereas far from equilibrium the process become wave-type.

At the initial loading stage  $t < t_R$  when the shear relaxation is still frozen on the back target surface  $t_r/t_R \rightarrow \infty, l_r/L \rightarrow 0$  the relationship (5) defines the elastic stress  $J_1(x,t) \rightarrow \rho_1 C^2$ . At the stage the impulse transport considers to be reversible. At the final stage during the long-time loading when the relaxation is completed and medium has already forgotten its initial stage  $t_r/t_R \rightarrow 0, l_r/L \rightarrow 0$ , Eq. (5) results the newtonian medium model

$$J_1(x,t) \rightarrow -\frac{4}{3} \rho_0^{-1} G^2 t_r \frac{\partial v}{\partial x}, \text{ where } \rho_0^{-1} G^2 t_r \equiv \mu \text{ is the shear viscosity coefficient. Near the}$$

hydrodynamic limit the impulse transport is irreversible because of the viscous energy dissipation into heat. In between the limits at finite spatiotemporal scales the wave and diffusive transport mechanisms appear not to be divided into additive parts in advance.

At the transition stage there arise another effects related to self-organization new internal structures at an intermediate scale level between macroscopic and atom-molecular one. Within the continuum mechanics framework this stage and the structure effects were always neglected because of the process division into elastic and hydrodynamic parts corresponding to the conventional medium model near equilibrium state.

## 6. Formulation of the problem on the shock-induced plane wave propagation

The wave propagation is characterized by three scale parameters:

1. Stress relaxation parameter  $\tau = \frac{t_r}{t_R}$ , defining the transport regime;
2. Retardation parameter  $\theta = \frac{t_m}{t_R}$ , defining the retardation of the maximal stress on the plastic front from the elastic precursor;
3. Nonlocality parameter (relaxation length)  $\varepsilon = \frac{C t_r}{L}$ , defining the contribution of the waveform evolution during its propagation.

New reference connected to the elastic precursor running at the constant longitudinal sound velocity  $C$  is introduced  $\zeta = \frac{1}{t_R} \left( t - \frac{x}{C} \right)$ ,  $\xi = \frac{x}{L}$ . In the reference the relationship between new coordinate derivatives  $\tau \frac{\partial}{\partial \zeta} \gg \varepsilon \frac{\partial}{\partial \xi}$  is conditioned by an evaluation  $\frac{\varepsilon}{\tau} \ll 1$ , resulted from the experimental conditions  $\frac{\varepsilon}{\tau} = \frac{C t_R}{L} \approx \frac{6 \cdot 10^3 \text{ m/s} \cdot 2 \cdot 10^{-9} \text{ s}}{10^{-2} \text{ m}} \approx 10^{-3}$ . The typical scale division considers being necessary to describe the structure self-organization, and allows essential simplification of the nonlocal model for the impulse transport in the new variables.

$$\frac{\partial \rho_1 / \rho_0}{\partial \zeta} - \frac{1}{C} \frac{\partial v}{\partial \zeta} + \frac{\varepsilon}{\tau} \frac{\partial v}{\partial \xi} = 0, \quad (6)$$

$$\frac{\partial v}{\partial \zeta} - \frac{1}{C} \frac{\partial C \Pi}{\partial \zeta} + \frac{\varepsilon}{\tau} \frac{\partial \Pi}{\partial \xi} = 0,$$

$$\begin{aligned} \Pi &= - \int_0^{Ct} d\xi' \int_0^\omega d\zeta' \Re(\zeta, \zeta'; \tau) \delta(|\xi - \xi'|) \left[ -\frac{\partial v}{\partial \zeta'} + \frac{\varepsilon}{\tau} \frac{\partial v}{\partial \xi'} \right] = \\ &= \int_0^\omega d\zeta' \Re(\zeta, \zeta'; \tau) \left[ \frac{\partial v}{\partial \zeta'} - \frac{\varepsilon}{\tau} \frac{\partial v}{\partial \xi'} \right], \quad \omega(\zeta) = \begin{cases} \zeta, & \zeta < 1 \\ 1, & \zeta \geq 1 \end{cases}. \end{aligned} \quad (7)$$

Here a new quantity is introduced  $\Pi(\zeta, \xi; \tau, \theta) = J_1(x, t) / \rho_0 C$ . The mass velocity is related to the shock velocity  $V_0$ . The coordinate  $\xi$  is counted from the back target surface which is at a distance  $L$  from the shock surface. The origin of the  $\zeta$ -axis is an instance when the elastic precursor reaches the back target surface and is registered by the device. Due to the scale division the spatiotemporal correlations in the integral kernel in Eq. (7) are also divided. So, only memory effects remain in the kernel whereas the spatial nonlocality is neglected. The following model expression for the memory function is used [23, 24]:

$$\Re(\zeta, \zeta'; \tau) = \exp \left\{ -\frac{\pi (\zeta - \zeta' - \theta)^2}{\tau^2} \right\}. \quad (8)$$

The parameters  $\tau(\xi), \theta(\xi)$  depend on the distance traveled by the wave. In general case, the functions  $\tau(\xi), \theta(\xi)$  are unknown due to the back influence of the wave propagation on the medium properties inside the wave.

## 7. Approximate solution for quasi-stationary wave propagation

The propagation of the shock-induced impulse of moderate intensity in condensed matter is

considered on the condition  $\frac{\varepsilon}{\tau} = \frac{Ct_R}{L} \ll 1$  that allows seeking of an automodel solution to the problem depending only on the wave coordinate  $\zeta$ . The solution describes quasi-stationary wave propagation accompanied by formation of the two-wave front. The waveform evolves with the model parameters  $\tau, \theta$  depending on the distance  $\xi$  traveled by the wave. Unlike conventional differential wave models, the solution should describe both relaxation of the elastic precursor and retardation of the plastic front. Till present there is no another consistent theory to explain waveform evolution in its propagation accounting the loading conditions.

The continuity equation (6) in the first order in the small parameter  $\frac{\varepsilon}{C} \ll 1$  results the

relationship between strain  $e$  and the mass velocity  $v = \frac{\rho_1}{\rho_0} = \frac{v}{C}$ . It must be noticed that

beyond the made assumptions it is better to use the mass velocity registered in real time in dynamic process instead of the concept of the strain to be reconsidered.

The impulse transport equation (7) with the members of the order  $\frac{\varepsilon}{\tau} \ll 1$  neglected takes a form

$$\frac{\partial v}{\partial \zeta} - \frac{\partial \Pi}{\partial \zeta} = 0, \quad \Pi(\zeta; \tau, \theta) = \int_0^\omega d\zeta' \exp \left\{ -\frac{\pi(\zeta - \zeta' - \theta)^2}{\tau^2} \right\} \frac{\partial v}{\partial \zeta'}. \quad (9)$$

Integrating Eq. (9) on the condition  $v(0) = 0$  results

$$v = \int_0^\omega d\zeta' \exp \left\{ -\frac{\pi(\zeta - \zeta' - \theta)^2}{\tau^2} \right\} \frac{\partial v}{\partial \zeta'}. \quad (10)$$

Equation (10) leads to a linear stress-strain relationship  $J_1 = \rho_0 C \Pi = \rho_0 C v = \rho_0 C^2 e$  like in the linear elasticity theory. In the elastic limit  $\tau \rightarrow \infty$ ,  $\zeta < 1$  Eq. (10) becomes an identity. However, the quantity  $e$  has the conventional meaning of the strain only in the elastic regime, whereas beyond the elastic limit the function  $e(\zeta; \tau, \theta)$  loses this meaning. Due to the integral kernel at finite parameters values  $\tau, \theta$  depending on the distance  $\xi = x$ , the velocity in the left side of Eq. (10)  $v(\zeta; \tau, \theta)$  differs from that under the integral in the right side  $v(\zeta; \tau_0, \theta_0)$ , where parameters  $\tau_0, \theta_0$  correspond to a previous waveform. It means that due to the parameters the spatial nonlocality remained in Eq. (10) where stress and strain relate to different spatial points. So, the integral operator in Eq. (10) plays a role of an evolution operator that describes the waveform evolution during its propagation in the medium. For elastic-plastic waves where the plastic deformation always retards from the elastic one arising simultaneously with the loading, the conventional treatment of the strain concept should be revised.

The integral Eq. (10) can be solved using by iteration method developed in theory of the special type nonlinear operators [30, 31]. Substitution into the right-hand side of Eq. (10) of an initial waveform  $v(\zeta; \tau_0, \theta_0)$  results an approximate solution to Eq. (10) in the first iteration. In general case the initial waveform is unknown. It can be experimentally measured only at a distance from the shock surface where a part of the initial information on the impulse exchange during the shock loading is already lost. Therefore the initial waveform assumes to be rectangular which corresponds to an infinite rate of the impulse exchange during the shock. However, in [15, 16] it had been demonstrated that the rate and duration of

the impulse exchange essentially influenced on the short impulse transport in condensed medium. In order to introduce the rate of the initial impulse exchange, the initial waveform assumes to be trapeze-type which corresponds to the finite acceleration  $\frac{\partial v}{\partial \zeta}$  induced by the constant force acting for a finite time interval  $t_R$ . For the velocity  $v$  and the variable  $\zeta$ , normalized to the shock characteristics  $V_0, t_R$ , the acceleration during the impact  $\frac{\partial v}{\partial \zeta} = 1$  equals to unit. Substitution of the initial acceleration into the Eq, (10) results an explicit automodel solution for the mass velocity wave front [23]:

$$v(\zeta; \tau, \theta) = \begin{cases} \frac{\tau}{2} \left( \operatorname{erf} \frac{\sqrt{\pi}(\zeta - \theta)}{\tau} + \operatorname{erf} \frac{\sqrt{\pi}\theta}{\tau} \right), & \zeta < 1, \\ \frac{\tau}{2} \left( \operatorname{erf} \frac{\sqrt{\pi}(\zeta - \theta)}{\tau} + \operatorname{erf} \frac{\sqrt{\pi}(1 - \zeta + \theta)}{\tau} \right), & \zeta \geq 1. \end{cases} \quad (11)$$

The solution (11) relates the stress inside running wave to the initial strain-rate during the shock. During the loading below the elastic limit the solution (upper expression) describes the relaxation of the elastic precursor. After the loading (lower expression) the solution describes the shear relaxation in plastic front as aftereffect due to the medium inertia, but not due to a plastic flow. The non-stationary two-wave front is forming without previous division of stress into elastic and plastic parts. Further it will be demonstrated that the approximate solution (11) adequately describes all the experimentally observed effects related to the quasi-stationary elastic-plastic wave propagation. Figures 8, 9 show the two-wave front formation according to the solution (11) at different values of the model parameters.

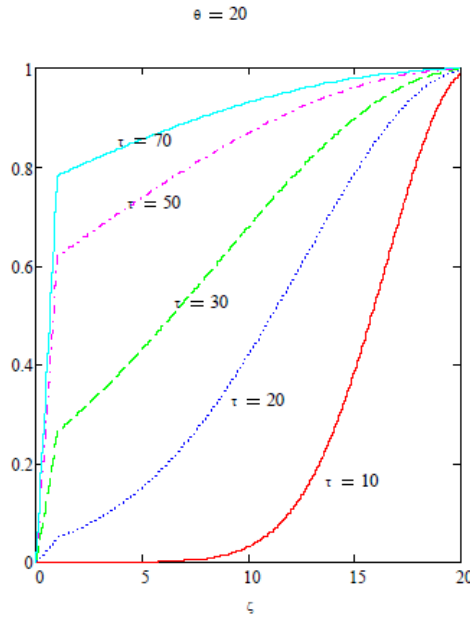


**Fig. 8.** Formation of the two-wave front at the fixed value of the retardation parameter  $\theta$  with decrease of the relaxation parameter  $\tau$ : (downwards)  $\tau = 70, 50, 30, 20, 10$ .

Depending on the parameters  $\tau, \theta$  the relaxation can be monotonous and nonmonotonous. Near the hydrodynamic limit with memory and retardation neglected, the stress after the loading begins to attenuate monotonously. At rather large values of parameters after the finished load beyond the elastic limit, the stress continues to grow due to inertia until it

reaches its maximal value  $\rho_0 C^{pl} V_0$ . It appears to be not plasticity but nonmonotonous relaxation. From experiments it is known that in the quasi-stationary wave propagation  $C^{pl} = C_0 = \text{const}$ . Then the stress  $\rho_0 C_0 v$  considers being the hydrodynamic pressure like in an ideal fluid which model underlies the ideal plasticity theory. However, the state of material inside the plastic front is too far from the hydrodynamic limit, and the concept of plasticity itself requires a different treatment. So, the second front of the wave should not be considered as plastic front but the relaxation one resulting from the retarding medium reaction to the high-rate loading. First, this assumption was made in [33]. Further we shall use the conventional terminology and call the second front plastic.

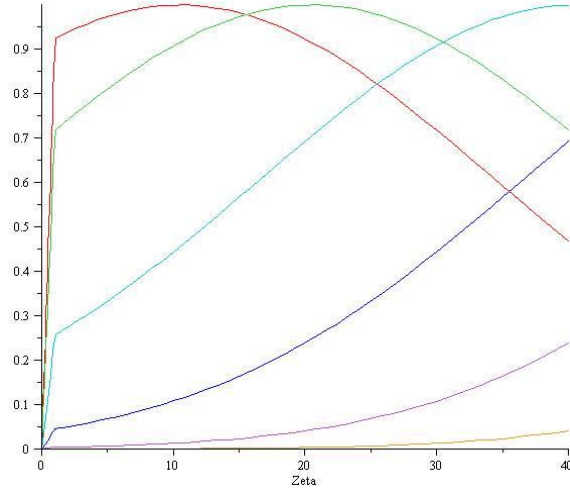


**Fig. 9.** Formation of the two-wave front at the fixed value of the relaxation parameter  $\tau$  with increase of the retardation parameter  $\theta$ : (downwards)  $\theta = 10, 20, 40$ .

## 8. Finite duration waveforms

Special features of the shock loading of solids are an unloading front and a plateau between the top of the plastic front and the unload beginning. These waveform features are conditioned by the interaction between an impactor of a finite length and a solid target. After the shock, one wave runs in the target, another propagates in the opposite direction inside the impactor at the longitudinal sound velocity  $C_{imp}$  corresponding to the impactor's material, and being reflected from its back surface, comes back into the target as the unloading front. Then the duration of the plateau is determined by a ratio  $2l_{imp} / C_{imp}$  where  $l_{imp}$  is a length of impactor. When the shear relaxation is already completed on the waveform top, the relaxation of the volume degrees of freedom is still frozen. It means that the rest waveform part after the shear relaxation propagates in the elastic regime without form changing, and the impactor does not exert a force on the target. When the unloading front (also consisting of its elastic precursor and following shear relaxation) comes, the impactor bounces off the target. So, the plateau appears due to the inertia of impactor's mass and not because of the plasticity effects. Figure 10 shows waveforms of the fixed duration at different values of the model parameters in the solution (11). With the retardation parameter increasing the plateau is shortened and can entirely disappear (so called "hydrodynamic attenuation" though it does not correspond to hydrodynamic behavior)

As distinct from elastic-plastic models [34-35], the elastic precursor in the unloading front within the proposed conception does not double, as far as no need first to compensate the medium compression on the plateau and then to unload medium till the elastic limit. During slow quasi-static loading stress and strain relate to a one spatiotemporal point (process

near equilibrium) whereas in shock-induced processes aftereffects and inertia play the main role. On the plateau the acceleration is absent  $\partial v / \partial \zeta = 0$ , and therefore the force is not applied. It should be noticed that the doubling of the elastic precursor had never been observed in experiments on the shock compression of different materials.

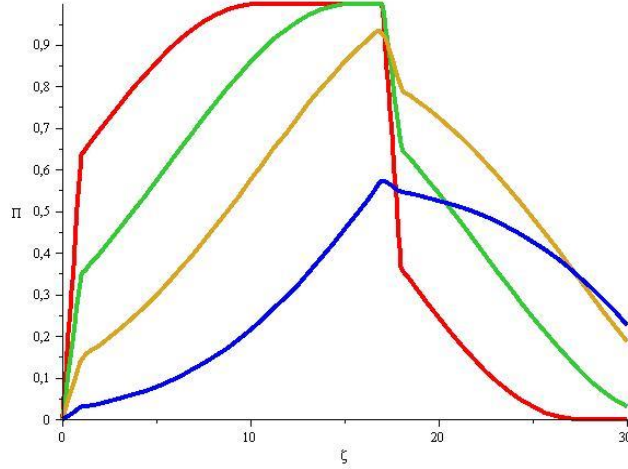


**Fig. 10.** Evolution of the finite duration waveform at the fixed value of the relaxation parameter  $\tau$  with increase of the retardation parameter  $\theta$ : (downwards)  
 $\theta = 10, \theta = 15, \theta = 20, \theta = 25$ .

Unlike the conventional approaches to the shock-induced processes [37-38], the plastic front is forming by the shear relaxation after the force of the shock proportional to the medium acceleration (or strain-rate) stops acting. The dependence of stress on the strain-rate is included into Eq. (10) and its solution (11) by means of the acceleration  $\frac{\partial v}{\partial \zeta} = 1$ . For quasi-static long-time loading at low strain-rates all aftereffects can be neglected as far as the medium reaction keeps up with the loading and the process history does not directly influence on it. The fundamental difference between quasi-static and shock loading can be seen on Fig. 11.

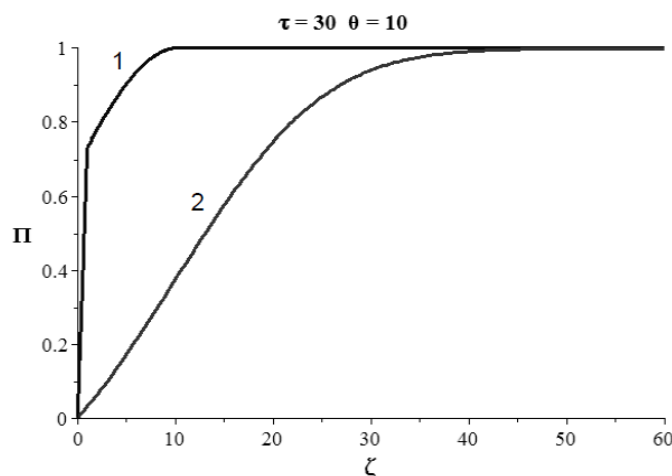


**Fig. 11.** Comparison of two waveforms of the same maximal amplitude induced by a shock (top) and quasi-static continuous loading (lower).

According to the solution (11), during the shock loading the elastic precursor reaches its maximal amplitude at the time  $t = t_R$  and after that the shear relaxation forms the plastic front. During the slow continuous loading at the constant strain-rate no two-wave front forms, one

front arises and beyond the elastic limit becomes plastic. Comparison of the two type loading at the same maximal amplitude shows that the strain-rate during the continuous loading should be approximately 25 times lower than during the shock. Because of the aftereffects in dynamic processes the time can not be excluded from the stress-strain relationship. Therefore, both the model of ideal plasticity with dependence on strain-rate neglected and all quasi-static stress-strain relationships recalculated using the results for simple compression of rods are not valid for high-rate shock-wave processes [35].

### 9. Interpretation of experimental waveforms in terms of the integral model

So, for the shock loading the initial strain-rate or acceleration plays an important role. However, at large values of the relaxation parameter  $\tau$  when the pulse duration much exceeds the loading time  $t_R$ , a simplifying assumption  $\frac{\partial v}{\partial \zeta} = \delta(\zeta)$  can be made. Then the relaxing plastic front is determined by the relaxation integral kernel

$$v(\zeta; \theta, \tau) \approx \exp \left\{ -\frac{\pi(\zeta - \theta)^2}{\tau^2} \right\}. \quad (12)$$

The maximal amplitude of the plastic front  $v_{\max}(\zeta = \theta) = 1$  is reached at the instant  $\zeta = \theta$ . It means that under the conditions the retardation parameter  $\theta$  determines the duration of the shear relaxation front with the elastic region being neglected. At low values of the parameter  $\tau$  the stress begins rapidly to attenuate immediately after the loading. Therefore, near the hydrodynamic limit the wave model (12) fails.

The maximal amplitude of the elastic precursor depends on the parameters  $\tau, \theta$  according to Eq. (12) as follows

$$A_e \approx \exp \left\{ -\left( \frac{\sqrt{\pi}}{\tau} \theta \right)^2 \right\}. \quad (13)$$

The relaxation of the elastic precursor occurs if the ratio  $\theta/\tau$  decreases. Experiments show that the relaxation completes when the amplitude reaches a fixed value  $A_e(\theta/\tau) = \text{const}$  which considers being an elastic limit according both to the material properties and to the loading conditions.

The approximate expression for the waveform (12) allows rather simple way to obtain the parameters  $\tau, \theta$  from the experimentally registered waveforms. The parameter  $\theta$  can be easily measured on the waveform and the parameter  $\tau$  can be calculated using the expression (13). Figure 12 demonstrates the experimentally measured dependences of the model parameters  $\tau, \theta$  on the target thickness. As far as the parameters  $\tau, \theta$  describe the changing medium reaction to the loading, their behavior allows a description of the waveform evolution during its propagation in a target.

### 10. Quasi-stationary regime of the waveform propagation

The dependence of the parameters  $\tau, \theta$  on the target thickness shown on Fig. 12 is obtained from the experimental data for quasi-stationary waveforms propagating in targets of aluminum alloy D16. For all five targets the elastic precursor amplitudes (13) have almost the same values ( $\exp\{-\pi\theta^2/\tau^2\} \approx \text{const}$ ). It means that in this regime the phase points  $(\tau(x), \theta(x))$  for all thicknesses lay along the straight line on the phase plane of the parameters  $(\tau, \theta)$ . Figure 13 shows two linear trajectories for two series of experiments on the shock

loading at the impact velocity in between the interval 200÷400 m/s and different target thicknesses for two materials: 30XH4M steel and Δ16 aluminum alloy. It can be seen that each phase point moves along the trajectory away from the coordinate origin during the wave propagation. Both trajectories are straight lines under different angles to axis depending on the material elastic limit for the range of impact velocities. Both lines can be extrapolated to the origin though there is no experimental data close to the origin and the parameters loose their meaning at low values  $\tau, \theta$ .

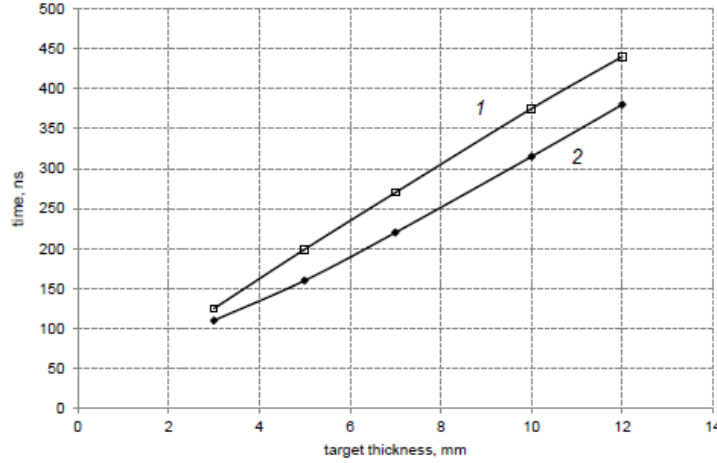


**Fig. 12.** Experimental dependencies of the relaxation parameter  $\tau$  (1) and the retardation parameter  $\theta$  (2) on the target thickness.

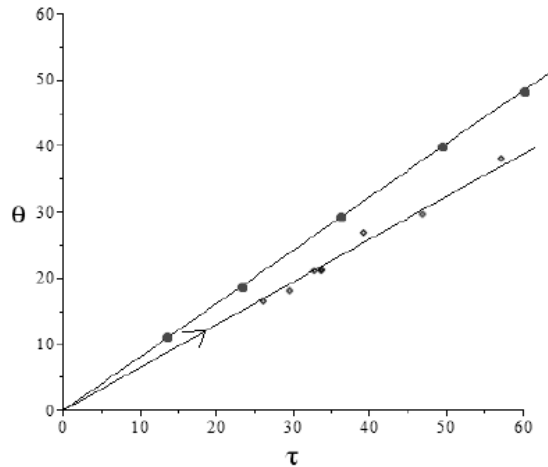


**Fig. 13.** Trajectories for two series of experiments on the shock loading at the impact velocity in the interval 200÷400 m/s and different target thicknesses for two materials: 30XH4M steel (lower) and Δ16 aluminum alloy (top).

According to the parameters, the trajectories the waveforms sprawl in the propagation, and the plateau of the plastic front retards increasingly from the elastic precursor. The rate of the retardation can be evaluated from experimental data as follows:  $C^{pl} = x / ((x/C) + \theta) \approx 5000 \text{ m/s} \approx C_0$ . It means that all experimental data correspond to the quasi-stationary regime of wave propagation. In quasi-stationary regime the plastic front moves at the constant velocity and the amplitude of the elastic precursor has a constant value in its propagation. The phase trajectories for the quasi-stationary wave propagation are beams along which phase points run away from the origin. Since the plateau of the plastic front propagates at the volume sound velocity, the shear relaxation is already completed whereas the volume

one is still frozen. The shear relaxation time (rise-time) grows in the wave propagation and the material state tends to elastic solid.

In the transition regime when the elastic precursor is still relaxing, the velocity of the plastic front is also not constant as well as the shear elastic module. It means that in general case it is incorrect to divide stress and strain into elastic and plastic parts in advance.

### 11. Anomalous velocity defect on the plateau of the plastic front

In experiments on the shock loading of solids with the increasing impact velocity an anomalous amplitude loss of the plastic front had been found out (Figs. 7, 8) which could not be explained only by the mechanical energy dissipation into heat. Slow diffusive (dissipative) mechanisms of energy and impulse transport in thin targets under short pulse loading have no time to develop. In the targets after nonstationary wave propagation new structures of an intermediate size between macro- and microscale had been observed. The experimentally found wave amplitude loss followed by the new structure formation apparently indicates to the multi-energy exchange inside the wave which does not yet descend to the microscale. At the mesoscale the energy is expended to the new internal structure organization [1-3]. Like in turbulent hydrodynamic flow, in experiments after the impact velocity threshold, mesoscopic rotational structures had been observed in the targets.

The impulse transport equation (7) contains derivatives on the slow variable corresponding to the impulse loss during the wave propagation

$$v - \int_0^\zeta d\zeta' \mathfrak{R}(\zeta, \zeta'; \tau) \left[ \frac{\partial v}{\partial \zeta'} - \frac{\varepsilon}{\tau} \frac{\partial v}{\partial \xi} \right] + \frac{\varepsilon}{\tau} \int_0^\zeta d\zeta' \frac{\partial \Pi}{\partial \xi} = 0. \quad (14)$$

If the factor  $\varepsilon / \tau \ll 1$  can be neglected (as in automodel solution) the amplitude of the plastic front is almost equal to the impact velocity. The case takes place at low impact velocities, and starting from some value of the velocity the amplitude loss begins to increase significantly. Account of terms with the factor  $\varepsilon / \tau$  in Eq. (7) violates the linear relationship between stress and mass velocity  $J_1 \neq \rho_0 C v$ .

In the first iteration the mass velocity amplitude defect  $\Delta v$  in the target of thickness  $L$  due to the amendment of the order  $\varepsilon / \tau \ll 1$  to the automodel solution  $v^0$ , determined by Eq. (11), can be approximately evaluated from Eq. (7) as follows [24, 36]

$$\Delta v = v^a - v = \frac{\varepsilon}{\tau} \int_0^\zeta d\zeta' \frac{\partial \Pi}{\partial \xi} \approx b \int_0^\zeta (\Pi(-L) - \Pi(0)) d\zeta'. \quad (15)$$

Figure 14 shows waveforms constructed accounting the velocity defect (15) at the different exchange parameters  $b$  compared to the experimental waveform at the same impact velocity.

It must be noticed that though the experimentally found growth of the wave amplitude defect with increasing of the impact velocity takes place, general dependences of the wave amplitude loss during the wave propagation in a medium are not entirely clear till present. In experiments the waveforms are registered in targets of different thickness at the approximately same impact velocities. Besides, the size of the laser spot generated by the interferometer to register the velocity of the free target surface is about 50÷300  $\mu\text{m}$ . It means that the registered velocity corresponds not to macroscale, and an additional averaging over experiment series is needed. So, a large scatter of the registered waveform amplitudes is observed. The greater impact velocities, the greater the scatter measurements with respect to the velocity defects. For the waveforms propagating in the quasi-stationary regime for low impact velocities the velocity defect has almost constant value which is about 10 % of the maximal amplitude in the plastic front [3].

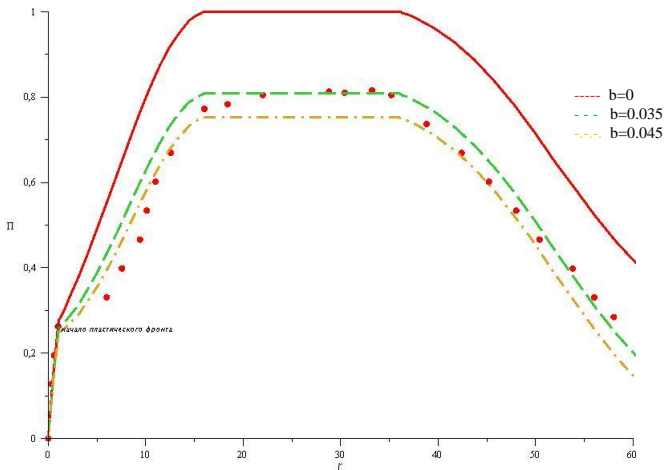


**Fig. 14.** Waveforms accounting the velocity defect (15) at the different exchange parameters  $b$  compared to the experimental waveform at the same impact velocity.

## 12. Discussion

Experimental research of the material response to the shock loading had revealed special features which distinguish dynamic processes from the quasi-static ones. From the standpoint of the conventional continuum mechanics the response seems to be anomalous due to the complex of accompanying relaxation and exchange processes which had never been included in conventionally used models. Aftereffects originated by relaxation and inertia make the response retarding. Impulse and energy exchange between different degrees of freedom induces a self-organization of new internal structures at the intermediate scale level between macro- and micro- scales. The internal structure, in turn, makes the response dispersed. The structure evolution leads to instabilities which cannot be predicted. All the features make the differential models in the framework of continuum mechanics inadequate for dynamic processes.

A need for a new theoretical approach able to describe the high-rate processes considering the whole complex of accompanying effects resulted in nonlocal theory of nonequilibrium transport. Application of the theory to the problem on the shock-induced wave propagation in solid materials allows an adequate explanation of the waveforms behavior during their propagation revealed in series of experiments on dynamic loading of different materials. It was found out that in dynamic processes stress and strain are related to different spatiotemporal points and cannot be correctly divided into elastic and plastic parts in advance. The so called plastic front appears to be the relaxation front and cannot be considered in the framework of hydrodynamic models. Only integral nonlocal models can describe all the special features inherent in the dynamic medium response to high-rate loading.

Until physicists use “rigid” differential models for high-rate nonequilibrium processes without involving of the internal structure evolution, the gap between fundamental science and practice would not be overcome.

## Acknowledgement

This work was supported in part (for Yu.I.M.) by Saint-Petersburg State University research grant 6.37.671.2013.

## References

- [1] J.R. Asay, LC. Chhabildas, In: *Shock Waves and High-Strain-Rate Phenomena in Metals. Concepts and Applications*, ed. by M.A. Meyers and L.E. Murr (Plenum Publishing Corporation, N.Y., 1981).

- [2] Yu.I. Meshcheryakov, S.A. Atroshenko // *International Journal of Solids and Structures* **29** (1992) 2761.
- [3] Yu.I. Meshcheryakov, A.K. Divakov, N.I. Zhigacheva, I.P. Makarevich, B.K. Barakhtin // *Physical Review B*. **78** (2008) 64301.
- [4] A.C. Koskelo, S.R. Greenfield, D.L. Raisley, K.J. McClellan, D.D. Byler, R.M. Dickerson, S.N. Luo, D.C. Swift, D.L. Tonk, P.D. Peralta, In: *Shock Compression of Condensed Matter - 2007. Proc. AIP-955* (N.Y., 2008), p. 557.
- [5] M.Yu. Gutkin, I.A. Ovid'ko, Yu.I. Meshcheryakov // *Journal de Physique III France* **3** (1993) 1563.
- [6] J.R. Asay, L.M. Barker // *Journal of Applied Physics* **45** (1974) 2540.
- [7] Yu.I. Meshcheryakov, A.K. Divakov // *Dymat Journal* **1** (1994) 271.
- [8] Yu.I. Meshcheryakov, A.K. Divakov, N.I. Zhigacheva // *International Journal of Solids and Structures* **41** (2004) 2349.
- [9] J.R. Asay, In: *Shock Compression of Condensed Matter-2001. AIP Conference Proceedings-620*, ed. by M.D. Furnish, N.N. Thadhani, Y-Y. Horie (Melville, N.Y., 2002), p. 26.
- [10] G. Ravichandran, A.J. Rosakis, J. Hodovany, P. Rosakis, In: *Shock Compression of Condensed Matter - 2001. AIP Conference Proceedings-620*, ed. by M.D. Furnish, N.N. Thadhani, Y-Y. Horie (Melville, N.Y., 2002) p. 557.
- [11] Yu.I. Meshcheryakov, A.K. Divakov, S.A. Atroshenko, N.S. Naumova // *Technical Physics Letters* **35** (2009) 1125.
- [12] Yu.I. Meshcheryakov, A.K. Divakov, N.I. Zhigacheva, B.K. Barakhtin // *International Journal of Impact Engineering* **57** (2013) 99.
- [13] J.J. Gilman, In: *Shock Compression of Condensed Matter-2001. AIP Conference Proceedings-620*, ed. by M.D. Furnish, N.N. Thadhani, Y-Y. Horie (Melville, N.Y., 2002), p. 36.
- [14] J.J. Gilman, In: *High Pressure Shock Compression of Solids VI. Old Paradigms and New Challenges*, ed. by Y-Y. Horie, L. Davison, N.N. Thadhani (Springer, 2002), p. 279.
- [15] V.A. Morozov, In: *Models of continuum mechanics. Proceedings of 14 Inter. school on models of continuum mechanics* (Ghukovskii, 1992), Vol. 1, p. 324.
- [16] O.D. Baizakov, V.A. Morozov, Yu.V. Sud'enkov, In: *Gas Dynamics and Thermo-exchange. Dynamics of uniform and nonuniform media* (Publ. Leningrad Univ., Leningrad, 1993), p. 9.
- [17] T.A. Khantuleva, Yu.I. Mescheryakov // *International Journal of Solids and Structures* **36** (1999) 3105.
- [18] T.A. Khantuleva, Yu.I. Mescheryakov // *Physical Mesomechanics* **2** (1999) 5.
- [19] T.A. Khantuleva, In: *Shock Compression of Condensed Matter - 1999. APS 1-56396-923-8/00*, ed. by M.D. Furnish, L.D. Chhabildas, and R.S. Hixon (2000), p. 371.
- [20] T.A. Khantuleva // *Journal de Physique IV France* **10** (2000) 485.
- [21] T.A. Khantuleva, In: *High-pressure compression of solids VI: old paradigms and new challenges*, ed. by Y. Horie, L. Davison, N.N. Thadhani (Springer, 2003), p. 215.
- [22] T.A. Khantuleva // *Chemical Physics* **24** (2005) 36.
- [23] T.A. Khantuleva, N.A. Serebryanskay // *Izvestiya VUZov, Fizika* **52** (2009) 165.
- [24] T.A. Khantuleva, *Nonlocal theory of nonequilibrium transport processes* (Publ. Saint-Petersburg Univ., Saint-Petersburg, 2013).
- [25] N.N. Bogolyubov, B.I. Sadovnikov, A.S. Shumovskii, *Mathematical methods of the mechanics of model systems* (Nauka, Moscow, 1989).
- [26] J.M Richardson // *Journal of Mathematical Analysis and Applications* **1** (2013) 12.
- [27] N. Ailavadi, A. Rahman, R. Zwanzig // *Physical Review A* **4** (1971) 1616.
- [28] D.N. Zubarev, S.V. Tishchenko // *Physics* **59** (1972) 285.

- [29] D.N. Zubarev // *Results of Science and Technics. Ser. Modern problems of mathematics* **15** (1980) 152.
- [30] S.A. Vavilov // *Doklady AN SSSR* **316** (1991) 22.
- [31] S.A. Vavilov // *Doklady AN SSSR* **323** (1992) 206.
- [32] A.L. Fradkov, *Cibernetical physics* (Nauka, Saint-Petersburg, 2003).
- [33] J.J. Gilman, In: *Shock Compression of Condensed Matter - 1991*, ed. by S.C. Schmidt, R.D. Dick, G.W. Forbes, D.G. Tasker (Elsevier Science Publishers B.V., 1992), p. 387.
- [34] J.N. Johnson, L.M. Barker // *Journal of Applied Physics* **40** (1969) 4321.
- [35] D. Wood // *Mechanics* 5(21) (1953) 150.
- [36] T.A. Khantuleva, Yu.I. Mescheryakov // *Physical Mesomechanics* **17(5)** (2014) 21.